



**HAL**  
open science

## **Soil dynamic stiffness and wave velocity measurement through dynamic cone penetrometer and wave analysis**

Quoc Anh Tran, Miguel Angel Benz Navarrete, Pierre Breul, Bastien Chevalier,  
Philippe Moustan

### ► **To cite this version:**

Quoc Anh Tran, Miguel Angel Benz Navarrete, Pierre Breul, Bastien Chevalier, Philippe Moustan. Soil dynamic stiffness and wave velocity measurement through dynamic cone penetrometer and wave analysis. XVI Congreso Panamericano de Mecánica de Suelos e Ingeniería Geotécnica, Nov 2019, Cancun, Mexico. pp.401-408, <10.3233/STAL190064>. <hal-02364587>

**HAL Id: hal-02364587**

**<https://hal.science/hal-02364587v1>**

Submitted on 25 Nov 2019

**HAL** is a multi-disciplinary open access archive for the deposit and dissemination of scientific research documents, whether they are published or not. The documents may come from teaching and research institutions in France or abroad, or from public or private research centers.

L'archive ouverte pluridisciplinaire **HAL**, est destinée au dépôt et à la diffusion de documents scientifiques de niveau recherche, publiés ou non, émanant des établissements d'enseignement et de recherche français ou étrangers, des laboratoires publics ou privés.



Distributed under a Creative Commons CC BY-NC 4.0 - Attribution - Non-commercial use - International License

# Soil Dynamic Stiffness and Wave Velocity Measurement Through Dynamic Cone Penetrometer and Wave Analysis

Quoc Anh TRAN<sup>a,1</sup>, Miguel Angel BENZ NAVARRETE<sup>a</sup>,

Pierre BREUL<sup>b</sup>, Bastien CHEVALIER<sup>b</sup> and Philippe MOUSTAN<sup>b</sup>

<sup>a</sup>Research, Development and Innovation Department, Sol Solution, France

<sup>b</sup>Institut Pascal, Civil Engineering, Clermont Auvergne University, France

**Abstract.** The main objective of this article is focus on the investigation methods to estimates two important geotechnical soil parameter that are modulus and shear wave velocity by using lightweight dynamic penetrometer called Panda 3®. Firstly, wave equation, decoupling and reconstruction implemented method are presented. Then, the approach to determine soil modulus as well as the soil shear velocity through shock polar curves in frequency domain will be presented. The obtained results are evaluated with other in – situ geotechnical tests. The analysis shows a good accuracy and quality of the measurements. In addition, due to the high resolution of the vertical measurements (around 200 measures/meter), the proposed device, Panda 3, could be a good tool in order to improve shallow soil characterization.

**Keywords.** Dynamic penetrometer, Panda3®, modulus, wave shear velocity, wave equation, spectral analysis, transfer function.

## 1. Introduction

Amongst the different in situ test methods, the dynamic penetrometer is one of the most used test worldwide; yet he did not take advantage of recent advances in electronics and computing and remains a rather old and rustic on a technical point of view. Nevertheless, the work done for the past 20 years on the lightweight dynamic penetrometer Panda® and especially the last research work on the Panda 3®, recent innovative instrumented dynamic cone penetrometer, showed that the integration of various sensors and a chain of acquisition and processing of the measured signals make it possible a complete description of the physical phenomenon of driving penetrometer and its interpretation. Numerous laboratory tests have shown the feasibility and validity of the results. However, very few tests were performed under real conditions in order to validate its use in the context of a geotechnical characterization campaign.

After a brief reminder of the Panda 3® principle and the used implemented method, we will present a new approach to determine soil modulus and wave velocity. This approach is founded on the transfer function (FFR) applied to Panda 3® tip measurements. Assimilating the cone tip of the penetrometer to a circular plate embedded

---

<sup>1</sup> Corresponding Author: Quoc Anh TRAN, Research, Development and Innovation Department, Sol Solution, France; E-mail: qatran@sol-solution.com.

in a semi-infinite elastic medium, it is possible to determine dynamic modulus  $E_{kd}$  as function of frequency according to Boussinesq method.

The results of a test campaign on an experimental field will be used in order to evaluate the reliability of measurements.

## 2. The Panda 3®: fundamental principle and signal analysis

In the early 1990s we witnessed in France the development of the lightweight penetrometer Panda® [1], the only dynamic variable energy penetrometer equipped with sensors to automatically record the drive energy during the survey. Driving is performed with a manual hammer that can be accelerated blow per blow according to the soil hardness. Recently, benefiting from the latest sensor technological developments, we are witnessing to the development of the third generation of Panda®, named the Panda 3®. Although the principle of the device remains basically the same, this is a device that makes it possible to obtain (by signal processing and wave decoupling blow per blow) both the soil dynamic resistance and additional parameters governing the settlement behaviour of the soil involved when the conical tip penetrate it, as shown by the load-penetration curve of the soil [2]. Moreover, the work carried out by [2, 4] shows that the spectral analysis (Frequency Response Function, FRF) of the cone reconstituted signals (strength, stress, speed, displacement...) is very powerful and useful if it is implemented to Panda 3® analysis.

The main principle of Panda 3® is as follows: during penetrometer driving et after one blow, deformations  $\varepsilon(t)$  and accelerations  $a(t)$  caused by the compression wave created by the shock, are measured in a section of the rod near to the anvil. In fact, when the hammer hits the anvil, a compression wave  $u(x,t)$  is created in the rods propagating downwards at  $ct$  speed the tip. When the wave  $u(x,t)$  arrives at the tip/soil interface, part of it is used to penetrate into the soil. A second part is reflected upwards into the rods. Roundtrips of the wave continue into the rods until the total energy contained in them is no enough to penetrate the soil. The propagation phenomenon of the wave  $u(x,t)$  in the rods of a dynamic penetrometer is described by *wave equation* (Eq. (1)). During its trips within the rods, the passage of the wave  $u(x,t)$  causes at any point  $x$  along the rods deformations  $\varepsilon(x,t)$  and particular velocity  $v(x,t)$  variations represented by the superposition of the two elementary waves. In fact, current solution used to solve wave equation is that obtained by the method of characteristics (Eq. (2)), represented by the superposition of the two elementary waves,  $u_d$  and  $u_r$ , respectively downwards and upwards waves within an elastic and homogeneous media:

$$\frac{\partial^2 u(x,t)}{\partial t^2} = c_t^2 \frac{\partial^2 u(x,t)}{\partial x^2} \quad (1)$$

$$u(x,t) = u_d(x - c_t t) + u_r(x + c_t t) \quad (2)$$

According to [2, 10], if downwards and upwards waves are known at a given  $x_A$  point on the rods, it is possible to calculate the dynamic quantities such as *strength, stress acceleration, velocity...* at any  $x$  point on the rods [6]. Moreover, in the most general case where the rods are considered as an elastic and/or viscoelastic, with a length  $L_r$ , wave propagation can be explained from its Fourier components [7]. In the BCGO method [6],

applied to the dynamic penetrometer driving, the stress  $\sigma(x,t)$ , strain  $\varepsilon(x,t)$ , velocity  $v(x,t)$  and displacement  $u(x,t)$  in a measurement point  $x$  along the rods can be expressed as follows :

$$\tilde{\varepsilon}(x, \omega) = A(\omega)e^{-i\varepsilon(\omega)x} + B(\omega)e^{i\varepsilon(\omega)x} \tag{3}$$

$$\tilde{\sigma}(x, \omega) = E^*(\omega) \left( A(\omega)e^{-i\varepsilon(\omega)x} + B(\omega)e^{i\varepsilon(\omega)x} \right) \tag{4}$$

$$\tilde{v}(x, \omega) = -\omega \left( A(\omega)e^{-i\varepsilon(\omega)x} - B(\omega)e^{i\varepsilon(\omega)x} \right) / \xi(\omega) \tag{5}$$

$$\tilde{u}(x, \omega) = -i \left( A(\omega)e^{-i\varepsilon(\omega)x} - B(\omega)e^{i\varepsilon(\omega)x} \right) / \xi(\omega) \tag{6}$$

where  $A(\omega)$  and  $B(\omega)$  are the Fourier components of the downwards and upwards waves,  $E^*(\omega)$  the complex Young's modulus and  $\xi(\omega) = k(\omega) + i\alpha(\omega)$  the complex wave number [4, 6, 7]. It can be noted that all the dynamic quantities can be obtained if the following values are known:  $E^*(\omega)$ ,  $\xi(\omega)$ ,  $A(\omega)$  and  $B(\omega)$ . By accepting that  $E^*(\omega)$  and  $\xi(\omega)$  are determined only by rods geometrical and material properties, downwards and upwards wave decoupling from raw records consists in determining the values of components  $A(\omega)$  and  $B(\omega)$ [6, 7] as shown below.

### 2.1. Tip reconstruction waves in Panda 3®

The current method used to signal reconstruction at the tip level of Panda 3® consists in calculate, from and after the upwards and downwards waves decoupling, the strength  $F_N(t)$  and velocity  $v_N(t)$  at any point of impedance change along the rods. Considering the rod as a perfect elastic material,  $F_N(\omega)$  and  $v_N(\omega)$  are calculated using the following expressions [4, 6, 8]:

$$\tilde{F}_N(x_n, \omega) = A(\omega)e^{-i\frac{\omega}{c_t}x_n} + B(\omega)e^{i\frac{\omega}{c_t}x_n} \tag{7}$$

$$\tilde{v}_N(x_n, \omega) = \frac{1}{Z_n} \left( A(\omega)e^{-i\frac{\omega}{c_t}x_n} - B(\omega)e^{i\frac{\omega}{c_t}x_n} \right) \tag{8}$$

$$\tilde{u}_N(x_n, \omega) = \frac{i\omega}{Z_n} \left( A(\omega)e^{-i\frac{\omega}{c_t}x_n} - B(\omega)e^{i\frac{\omega}{c_t}x_n} \right) \tag{9}$$

With  $x_n$  the distance between the sections  $n-1$  and  $n$  considered,  $c_t$  the speed wave propagation and  $Z_n$  the rods mechanical impedance ( $Z_n = E_t A_t / c_t$ ). In time domain, the strength  $F_N(t)$  and velocity  $v_N(t)$  can be written [9-10]:

$$F_N(t) = \frac{1}{2}(F_{N-1}(t + \Delta t_{n-(n-1)}) + F_{N-1}(t - \Delta t_{n-(n-1)})) + \frac{1}{2}Z_n(v_{N-1}(t + \Delta t_{n-(n-1)}) - v_{N-1}(t - \Delta t_{n-(n-1)})) \quad (10)$$

$$v_N(t) = \frac{1}{2}(v_{N-1}(t + \Delta t_{n-(n-1)}) + v_{N-1}(t - \Delta t_{n-(n-1)})) + \frac{1}{2Z_n}(F_{N-1}(t + \Delta t_{n-(n-1)}) - F_{N-1}(t - \Delta t_{n-(n-1)})) \quad (11)$$

with

$$\Delta t_{n-(n-1)} = (x_{n-1} - x_n)/c_n \quad \text{et} \quad Z_n = E_n A_n / c_n .$$

Once the penetrometer conical tip signals have been reconstructed, the dynamic load-penetration curve is plotted for each blow and different strength and strain parameters can be determined [2, 11]. Moreover, some work has been done on the application of this new technique implemented on the dynamic penetrometer to the soil characterisation [2, 12]. Nevertheless, no work has addressed the issue of the dynamic module as well as wave velocity of soil and the relationship it could have with the load frequency imposed on the soils.

## 2.2. Soil dynamic modulus and wave velocity measurements using FRF

The FRF is a transfer function expressed in the frequency domain. It allows the spectral response of conical tip signals (*acceleration, speed and displacement*) to be analyzed as a function of the input or imposed load (force/strength). By normalizing the output signals with respect to the input signal, the characteristics and the response of the dynamic penetrometer system, such as stiffness, can be determined.

The dynamic modulus  $E_{K_d}(f)$  will thus be determined according to this approach and from the raw records made by the Panda 3®. For each blow the strength, acceleration, velocity and cone penetration are calculated (Eqs.7-11). The FRF known as "dynamic rigidity"  $K_d(f)$  is then calculated by considering the strength  $F(f)$  as the input load and the penetration  $S(f)$  as the output signal. Moreover, the FRF called "*admittance or mobility*" can also be calculated (Eq. (13)) in order to determine the dynamic mechanical impedance as well as deduce the compression wave velocity (Eq. (14)).

$$K_d(f) = \frac{F(f)}{S(f)} \quad (12)$$

$$Z_d(f) = \frac{F(f)}{V(f)} \quad (13)$$

$$V_p(f) = \frac{Z_d(f)}{A^* \gamma} \quad (14)$$

$$V_s = V_p \sqrt{\frac{1-2\nu}{2(1-\nu)}} \quad (15)$$

By assimilating the penetrometer conical tip to a circular embedded plate in a semi-infinite elastic medium (Boussinesq's approach), it is possible to compute the complex deformation modulus  $E_{K_d}(f)$  as a function of frequency  $f$  (Figure 1.a). This curve allows

to identify the range of frequency where the  $E_{Kd}(f)$  is linearly proportional to the frequency, as shown in (Figure 1.a). This frequency range depends on the nature and compaction state of the soil. The more rigid the soil, the greater the extent of this proportionality range. It is therefore important to determine the maximal and minimal limits of frequency defining this range. To do this, the top (measurement point) and bottom (conical tip reconstructed signal) curves of  $E_{Kd}(f)$  (Eq. (12)) are calculated and plotted in order to determine the minimum  $f_{min}$  and maximum  $f_{max}$  values of frequencies. Minimal value  $f_{min}$  depends on the characteristics of the data acquisition system (24Hz). Maximal frequency  $f_{max}$  is determined in our approach as the frequency where the value of  $E_{Kd}(f)$  at the top and bottom begins to diverge. The values of the dynamic modulus of the soil  $E_{Kd}$  are therefore calculated for these two limits frequencies. A third  $E_{Kd}$  value is also calculated; it represents the average value of the dynamic modulus between  $f_{min}$  and  $f_{max}$ .

On the other hand, by using the same approach to the determination of the dynamic modulus  $E_{Kd}$ , dynamic impedance is also calculated. By considering the force  $F(f)$  as the input excitation and the velocity  $V_p(f)$  as the output signal at the tip level (Eq. (13)). Considering same mobility behavior of medias at the tip/soil interface, the wave velocity of the soil can thus be determined as a function of frequency by dividing the dynamic impedance  $Z_n(f)$  by the tip section  $A$  and the soil density  $\gamma$  (Eq. (14)).

Figure 1.b shows an example of the compression wave velocity curves  $V_p(f)$  calculated at the top and bottom of penetrometer for different blows. In this article, we will only present the compression wave velocities  $V_p$  and shear wave velocities  $V_s$  which are calculated using the shock polar [13] as well equation presented below. In this approach, for each blow the peaks values of the downwards and upwards waves recorded into the rods in the range of time from  $t_o$  to  $t_o+2L_{rod}/c$  allows to calculate the soil compression wave velocity  $V_p$  [2, 3, 13]. The shear wave velocity  $V_s$  is calculated from the expression (Eq. (15)) and by assuming a value of  $\nu$  equal to 0.33 (*Poisson's coefficient*).

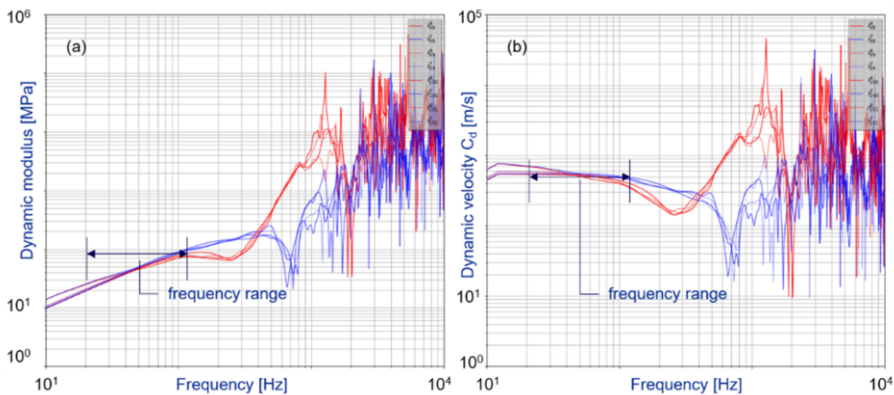


**Figure 1:** Example of the evolution of the dynamic modulus  $E_{Kd}$  (a) and the compression wave velocity  $V_p$  as a function of frequency  $f$ . Red lines represent the signals recorded at the top (measurement section), while the blue lines represents the signal reconstructed at the bottom level (penetrometer tip)

### 3. In-situ test validation

The experimental site is located south of the city of Castelló d'Empúries in the province of Girona in Spain (Figure 2). It is located in an alluvial plain forming a Mediterranean deltaic fill. At depth there is an alternation of sandy horizons and silty and clayey layers, with gravelly passages [14]. On this site, an important number of geotechnical testing were carried out : 8 Panda 2® holes ( $Z_{final} \sim 8.0m$ ), 6 Grizzly 3® ( $Z_{final} \sim 15.0m$ ) [3], 1 MASW 2D profile and 6 Panda 3® ( $Z_{final} \sim 8.0m$ ). Existing geotechnical test on the site are: 2 CPTu, 1 pressuremeter test (PMT) and 2 seismic Marchetti dilatometer (sDMT).

In order to evaluate reliability of the dynamic modulus  $E_{Kd}$  determined by using this new approach based on FFRs functions, a comparison between the Panda 3® and pressuremeter test PMT is presented. Considering that the range of deformation in the soil caused by the pressuremeter test is above of  $10e^{-4} - 10e^{-3}$ , and the loading speed remains low, the value of  $E_{Kdmin}$  determined for frequency  $f = 24.4 \text{ Hz}$  is considered. Both modulus,  $E_{kd}$  and  $E_M$  are plotted on the same graph.

Moreover, strength parameter are also compared. Panda 3® cone resistance  $q_d$  are compared with CPT  $q_c$  results, as shown in Figure 3.a.

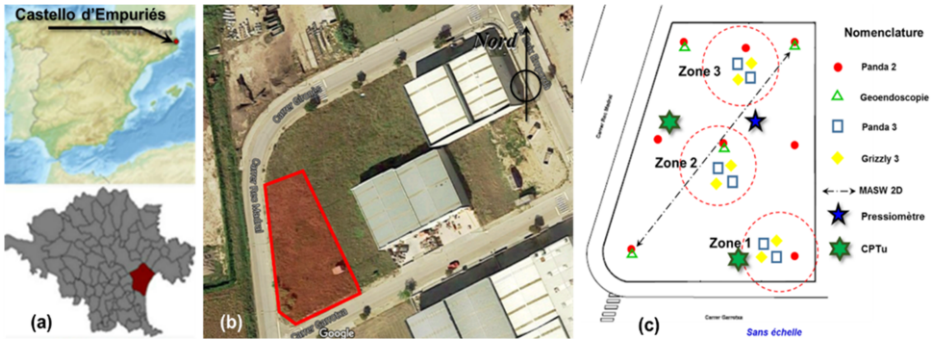


Figure 2. Castelló d'Empúries experimental site (Girona, Spain) (a) Geographical location of the site, (b) Castelló d'Empúries test site (Google earth©) and (c) Drilling layout scheme.

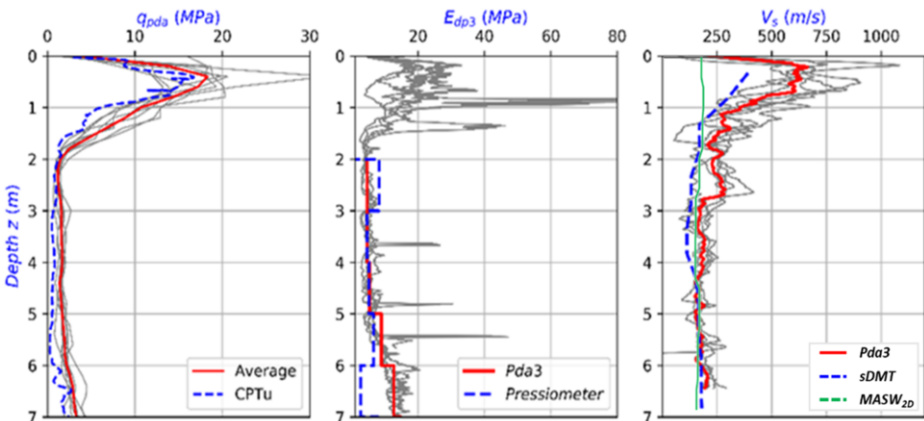


Figure 3. In-situ test campaign: comparative tests. (a) Peak resistance profiles  $q_d$ : Panda3® vs CPTu; (b) Module profiles ( $E_{Kd_{min}} / E_M$ ): Panda 3® vs PMT, and (c) Shear wave velocity profile: Panda 3®, MASW2D and sDMT. A very good correspondence is observed between the different tests.

Figure 3-a shows the results obtained on site in terms of cone resistance obtained in site through Panda 3® and CPT tests. The cone resistance profiles  $qd(z)$  obtained from the six Panda 3® carried out are presented in grey line. The average profile of  $qd(z)$ , calculated every 100mm increments, is presented in red line. Moreover, the results obtained with the CPT tests are also presented in blue line. They are compared with each other on the same graph. We note a good agreement of both profiles.

Figure 3-b shows the comparison of the Panda 3®determined modulus with the pressuremeter test (PMT). The  $E_{k_{dmin}}$  profiles obtained from the six Panda 3® test are presented in grey line. The average value, calculated in the windows with 1.0 m width, is presented in the same graph in red line in order to facilitate the comparison with PMT. Indeed, one of the big difficulties when comparing the results obtained with PMT tests is related to the low resolution of vertical measurements (1 meas./meter); while the Panda3® sampling frequency is about 200 measures/meter, which facilitates the statistical analysis of the raw data. PMT results are superimposed and plotted in a blue line on the same graph (Figure 3.b). No PMT measurements were made until 2.0m depth, because a very compact backfill is presented on site. A very good correspondence between the values obtained is also noted, especially between 2 and 6 meters deep. Above that, PMT measured  $E_M$  value is much lower, which seems strange. Indeed, for this layer, the measured cone resistance with CPT and Panda, and with DMT, increase. A decrease in the modulus values suggests either a variability in soil characteristics or an error in the measurement at this level.

In Figure 3-c a comparison between wave velocity  $V_s$  determined by different methods: *MASW2D*, *sDMT* and *Panda 3®* is also presented. Panda 3® profiles of  $V_s(z)$  (calculated according to Eq. (14)-(15)) obtained from the six test performed on site are presented in grey line. Average value is plotted in red line. The  $V_s(z)$  profiles measured with the *sDMT* and *MASW2D* are also presented in blue and green lines respectively. Despite the different resolution of measurement between each compared method, it can be seen that there is also a very good agreement between all profiles  $V_s(z)$  measured on site.

#### 4. Conclusion

The works presented by [2, 3, 4, 11, 12] proposes a new soil characterization technique associated to the dynamic variable energy penetration test, the Panda 3®.

Reliability of the measurements was carried out with the device; combined with the simplicity, rapidity and high resolution of the obtained signal, make it an interesting alternative for the geotechnical engineer in order to assess soil dynamic parameter.

In this article a new approach to determine soil's dynamic modulus and wave velocity from transient measurements made with dynamic penetrometer Panda 3® was presented. To do this, we applied to the penetrometer tip reconstructed signal a spectral analysis and the transfer functions (FRF). *Dynamic rigidity* and *mobility FRF curves*, was analyzed and the values of the dynamic modulus  $E_{k_d}(f)$  as well as compression wave speed  $V_p(f)$  of soil are determinate from shock polar curves.

To evaluate reliability of measurement, an in-situ test campaign was carried out in an experimental site, located close to Girona (Spain). In-situ comparative tests shown a good relationship between the results obtained with Panda 3® technique (elastic modulus, wave velocity, dynamic cone resistance) and those proposed by other classical geotechnical techniques (CPTu, PMT, MASW2D, sDMT...). In addition, the Panda 3®

repetitively, sensitivity and reliability was shown, and its great quantity of data make easy to improve the soil layer characterization by using statistical data analysis [14]. We have highlighted the quality and richness of the measurements.

## References

- [1] Gourvès Roland. *Pénétromètre dynamique léger à énergie variable*, LERMES CUST, University Blaise Pascal, Clermont-Ferrand, France, 1991.
- [2] Benz Navarrete, M. A. *Mesures dynamiques lors du battage du pénétromètre Panda2®*, Clermont Ferrand, France: Thèse de l'Université Blaise Pascal, 2009.
- [3] Escobar, E. et al. Dynamic characterization of the supporting layers in railway tracks using the dynamic penetrometer Panda3®. *Proc. Eng.*, **143** (2016), 1024-1033.
- [4] Tran, Q. A. et al. Modeling of light dynamic cone penetration test – Panda3® in granular material by using 3D discrete element method. *Proceedings of 8th International conference on micromechanics of granular media, Powder and Grain* (2017).
- [5] Calvente, R. M. et al. Non-destructive control methodology for micropiles based on low strain dynamic load test. Buenos Aires, Argentina, *Fundamentals to applications in geotechnics*. D. Manzanal and A.O. Sfriso (Eds.), 2015.
- [6] Bussac, M., Collet, P., Gary, G. & Othman, R. An optimisation method for separating and rebuilding one-dimensional dispersive waves from multi-point measurements, Application to elastic or viscoelastic bars. *J. Mech. Physics and solids* **50** (2002), 321–350.
- [7] Lodygowski, T & Rusinek, A. *Constitutive relations under impact loadings*, CISM International centre for mechanical sciences, Udine, 2014.
- [8] Lundberg, B. & Henchoz, A. Analysis of elastic waves in non-uniform rods from two-point strain measurement. *Experiment. Mech.*, **17** (1977), pp. 213-218.
- [9] Karlsson, L., Lundberg, B. & Sundin, K. Experimental study of a percussive process for rock fragmentation. *International Journal of Rock Mechanics and Mining Sciences and Geomechanics Abstracts*, 1(26) (1989), 45-50.
- [10] Casem, D., Fourney, W. & Chang, P. Wave separation in viscoelastic pressure bars using single-point measurements of strain and velocity. *Polymer testing*, **22** (2003), 155-164.
- [11] Benz Navarrete, M. A. et al. Mesures dynamiques lors du battage pénétrométrique–détermination de la courbe charge-enfoncement dynamique en pointe, *In Proceedings of the 18th International Conférence on Soil Mechanics and Geotechnical Engineering*, Paris, France (2013).
- [12] Benz Navarrete, M. A. et al. Détermination de la raideur dynamique des plateformes ferroviaires à l'aide de l'essai pénétrométrique Panda3®, *2ème Symposium International en Géotechnique Ferroviaire – Georail*, Marne la Vallée, Paris, France (2014).
- [13] Aussedat G. *Sollicitations rapides des sols*. Thèse de doctorat, Faculté de sciences de l'Université de Grenoble, 1970.
- [14] Sastre et al. Exploitation of dynamic cone penetrometer signal to obtain a ground model. *Journées Nationales de Géotechnique et de Géologie de l'Ingénieur*, Champs sur Marne, (2018).